Microelectronics Reliability 95 (2019) 48–51

Contents lists available at ScienceDirect

Microelectronics Reliability

journal homepage: www.elsevier.com/locate/microrel

Reliability and lifetime estimations of GaN-on-GaN vertical pn diodes

B. Rackauskas[a,*], M.J. Uren[a], T. Kachi[b], M. Kuball[a]

[a] Centre for Device Thermography and Reliability (CDTR), H.H. Wills Physics Laboratory, University of Bristol, Bristol BS8 1TL, UK
[b] Institute of Materials and Systems for Sustainability, Nagoya University, Furo-cho, Chikusa-ku, Nagoya 464-8601, Japan

ARTICLE INFO

Keywords:
Reliability
Lifetime
GaN-on-GaN
MTTF
Vertical pn diode

ABSTRACT

This work presents the first lifetime estimation of vertical GaN-on-GaN pn diodes using a step stress measurement technique with analysis not previously applied to GaN. The failure mechanism is surface breakdown, indicating that the lifetime is not yet limited by intrinsic material properties but by device design. As such, the mean time to failure depends on the peripheral length of the device. An estimated operating MTTF of 10 years at a reverse bias stress of 260 V was calculated for a 126 μm diameter diode.

1. Introduction

Power electronic systems have begun to adopt GaN based power devices in recent years based on their ability to operate at high power with high efficiency. These lateral devices are replacing their Si equivalents due to the superior material properties of GaN, specifically, the high breakdown field and high 2DEG mobility [1]. There is however increasing focus on developing vertical GaN devices because of the potential for increased power density, capability of higher voltage operation, and the possibility of approaching theoretical maximum breakdown fields in the absence of surface effects. Vertical GaN-on-Si devices offer the advantages of low cost and easy integration with existing foundries, which has motivated research on these devices with some success [2]. However, GaN devices on bulk GaN substrates are much more suited for vertical device architectures since GaN-on-Si and other available substrates have a higher vertical leakage due to the increased dislocation density. Recent developments in the growth of bulk GaN has led to a drop in the cost of substrates and GaN-on-GaN devices have become more economically viable. Already, bulk GaN pn diodes with breakdown voltages in excess of 4 kV and simultaneously low on-resistances below 3 $m\Omega cm^{-2}$ have been reported [3,4]. Some groups have also reported avalanche breakdown indicating suppression of defect related breakdown [5–7]. Despite this progress, there are only a few published reliability studies on these devices [8–11] and no lifetime estimations. Breakdown in Si oxides has been attributed to the formation of a percolation path formed of point defects which are randomly generated in high field stress conditions [12]. The failure of AlGaN/GaN HEMTs has been shown to follow the same failure distributions indicating a similar failure mechanism occurs in GaN [13]. Here we use an accelerated lifetime test based on step stress measurements to show the failure is; 1) due to the surface despite a vertical device design and therefore 2) the mean time to failure (MTTF) depends on the length of the periphery. Based on this, we predict a MTTF of each device size and discuss the reason for the periphery dependency.

2. Devices

The pn diodes in this study were circular devices with the cross-section shown in Fig. 1. The GaN device layers were grown by MOCVD on an HVPE GaN substrate. Starting with an n^+ layer grown on the substrate, a 5 μm n^- drift layer was grown with a Si density of 3×10^{16} cm^{-3}. The p^+n^- junction was created by the growth of 0.5 μm of p-GaN doped with 4×10^{19} cm^{-3} of Mg. A photoresist erosion and dry etch process was used on the p-GaN surface to create the final truncated conical structure which was left unpassivated. This edge termination by a bevel of 7°–10° reduced the surface electric field compared to that in the bulk [14]. With a negative bevel angle, as is the case here, the surface electric field is lower than the bulk provided the angle is sufficiently small. Contacts of Ni/Au and Ti/Al on the p- and n-GaN respectively were fabricated from a recipe originally developed for LEDs and which gave high quality Ohmic characteristics. The devices had an ideality of 1.4 and a reverse leakage current in the order of pA at −200 V. Further details of the leakage properties of the devices are included in another work [15].

3. Experimental

Step stress measurements were carried out by increasing the reverse

* Corresponding author.
E-mail address: ben.rackauskas@bristol.ac.uk (B. Rackauskas).

https://doi.org/10.1016/j.microrel.2019.02.013
Received 11 October 2018; Received in revised form 16 January 2019; Accepted 28 February 2019

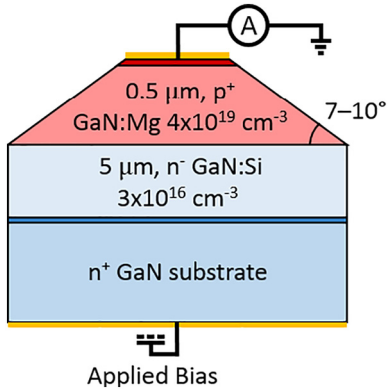

Fig. 1. A schematic of the device cross-section and wiring diagram. The bias was applied to the substrate and the current measured at the p terminal on the surface.

bias stress by 5 V every 60 s, starting from 0 V. This method offers a faster measurement time compared to conventional time dependent dielectric breakdown (TDDB) techniques since the stress voltage is gradually increased, resulting in a bounded time to failure. Three device sizes were studied; large, medium and small, with diameters of 451, 276 and 126 µm respectively. Twelve devices of each size were measured to generate the failure distributions with a failure criterion of 10 mA leakage current (6–80 Acm^{-2}). The bias was applied using a Keithley 2657A and the current was measured with a Keithley 4200 configured with a pre-amplifier giving 10 fA resolution.

4. Results

The currents during the step stress measurement of the twelve small devices are shown in Fig. 2, with the stress condition shown on the right axis. At low leakage currents, spikes are visible when the voltage is stepped up due to a spike in the displacement current $\left(C\frac{dV}{dt}\right)$. The leakage in this low current regime has been attributed to threading dislocations [15]. At higher currents, exceeding the pA level, a source of noise was introduced with distinct steps both up and down. These small devices began to fail after ~2800 s at voltages greater than 230 V. The cumulative distribution function (CDF) of these failures, indicating the fraction failed, is shown in Fig. 3. After failure, all devices showed visible signs of surface breakdown, an example of which is inset to Fig. 3.

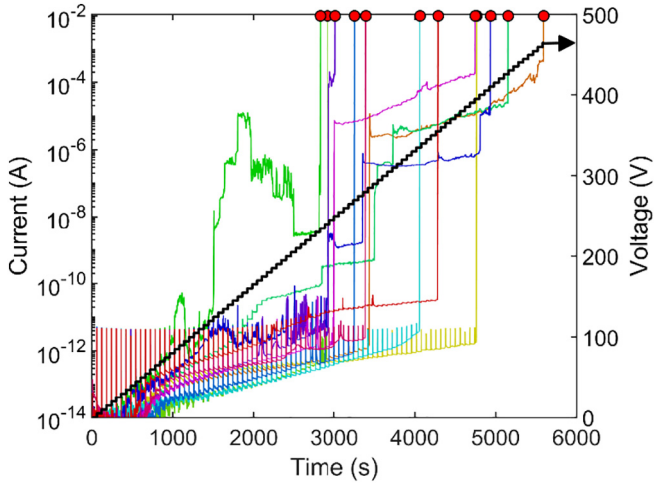

Fig. 2. The current during the step stress measurements of the small devices. The stepped stress voltage is shown on the right axes and the time of failure is indicated by the circles.

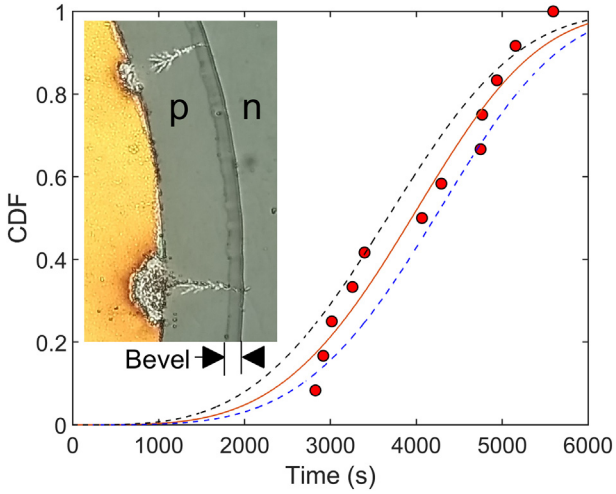

Fig. 3. The cumulative distribution of the small device failures in Fig. 2 (circles). This is fitted with the step stress Weibull distribution and the 95% confidence intervals are shown as dashed lines. The fit parameters are shown in Table 1. An optical plan-view image is inset showing surface failure across the pn junction.

5. Fitting

During a conventional TDDB measurement, devices are stressed at a constant voltage and their failure can often be fitted with a Weibull distribution of the form

$$F(t;V_i) = 1 - \exp\left(-\left(\frac{s}{s_0}\right)\left(t\left(\frac{V_i}{V_0}\right)^p\right)^\beta\right) \quad (1)$$

where V_0, p and β are fitting parameters, V_i is the (constant) stress voltage, and t is the time into the stress [16]. The factor s/s_0 is used to rescale the distribution based on the size of the device. A larger device is more prone to failure since it can be divided up into multiple statistically independent units and failure of any one unit leads to the failure of the entire device. Where failure is in the bulk, the unit will be a unit of area, and the rescaling will be a normalisation of the total device area. However, in the measurements reported here, failure is always surface breakdown on the periphery of the device. Therefore, the unit is a unit of length and the distribution must be rescaled based on the length of the periphery. In the following analysis, s is the device diameter and s_0 is the diameter of the large device.

Since in a step stress measurement the voltage is not constant, the failure data does not follow the typical Weibull distribution in Eq. (1). However, an appropriate distribution can be calculated (described in detail elsewhere [16]) by a piece-wise construction, treating each step as a constant stress TDDB measurement. For a given set of parameters (V_0, p, β), the step stress Weibull distribution is constructed one step at a time, where V_i is now the stress voltage of the i^{th} step. During the first step, the CDF proceeds according to the constant stress distribution of Eq. (1), $F(t, V_1)$. When the voltage steps up, the step stress distribution continues along the new constant stress distribution of the new voltage, $F(t, V_2)$, but starting from a later time to account for the cumulative stress already experienced by the devices. A good measure of how much cumulative stress a device has experienced is the fraction of devices that have already failed. Therefore, the step stress distribution is continued by moving onto $F(t, V_2)$ at the same value of F that it left off from $F(t, V_1)$. Fitting of this calculated step stress distribution to the measurement data was performed using a least squares algorithm, after which the 95% confidence interval of each parameter was evaluated by varying one parameter at a time. The result of this fitting to the data of the small devices is shown in Fig. 3 with the fit parameters for all three device sizes shown in Table 1.

Table 1
The fit parameters for the step stress Weibull distributions for each of the three device sizes. In brackets are the 95% confidence intervals. The average parameter set (weighted by the uncertainty) is shown in the final row.

Diameter (μm)	V_0	p	β
126 (small)	327 (13)	20.9 (4.1)	0.176 (0.018)
237 (medium)	312 (9.3)	28.7 (5.8)	0.151 (0.025)
451 (large)	324 (7.3)	31.7 (3.9)	0.190 (0.045)
Average	320.5	26.98	0.1695

6. Discussion

Each of the three fits has a different set of parameters, however, the 95% confidence limits of β and V_0 all overlap. Therefore, these parameters are not statistically significantly different. Considering the p parameter, the largest difference between the parameters is $\Delta p = 10.8$. Since the fits are independent, the variance of Δp is the sum of the p variances; $\sigma^2 = 6.5$. The 95% confidence interval is therefore $\Delta p \pm 1.96 \times \sigma^2$ (since 95% of the area of a normal distribution is within 1.96 standard deviations of the mean). This interval encompasses zero which means the difference in p is not statistically significantly different from zero. This observation that the three parameter sets do not differ significantly from each other after rescaling by the periphery length confirms that the breakdown is periphery dependent and not area dependent. An average parameter set was calculated using the uncertainty as a weighting. The consequence of using a constant parameter set for all three devices is that the periphery scaling factor is the only difference between the distributions. The step stress distributions plotted with the average parameter set are shown in Fig. 4 where there is a good agreement with all of the data sets.

The Weibull parameters and Eq. (1) can then be used to calculate the MTTF under constant stress. These results indicate the device lifetime depends only on the voltage and the periphery length. The MTTF of the Weibull distribution is calculated by

$$\mathrm{MTTF}(V;s) = \left(\frac{V_0}{V}\right)^p \left(\frac{s_0}{s}\right)^{\frac{1}{\beta}} \Gamma\left(1+\frac{1}{\beta}\right) \tag{2}$$

where Γ is the gamma function. This equation is plotted in Fig. 5 for the three devices with the dependence of the MTTF on device diameter shown in the inset. For a MTTF of 10 years, this corresponds to an operating voltage of 260 V for the small devices falling to 196 V for the largest devices. The high variability in device failure means the Weibull distributions have a small β parameter and consequently, there is a very short predicted 1% failure time of only tens of hours at just 100 V for the small devices.

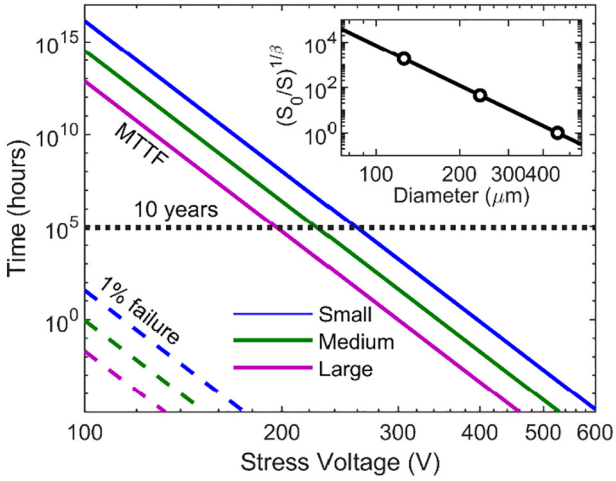

Fig. 5. The mean time to failure and the 1% failure time under constant stress are shown in solid and dashed lines respectively, predicted from the Weibull parameters. The horizontal dotted line corresponds to a lifetime of 10 years. Inset is the dependence of the MTTF on the diameter.

The steps in the leakage currents before failure are likely to be random telegraph noise as surface leakage is modulated by the changing occupancy of surface states or by configurational changes [17,18]. Simulations of these devices shown in Fig. 6 reveal a concentration of the electric field at the base of the device bevel. Considering the theory of failure by the random field induced generation of point defects, the defect generation rate is dependent on the electric field [19]. Thus, this increased electric field would increase the generation of point defects and the probability of creating a percolation path resulting in breakdown. This is consistent with the observed surface breakdown on the bevel after failure and explains the dependence on periphery. Equally, as each unit length of the periphery is independent of the next, the probability of failure is directly proportional to the total length of the periphery. In a commercial device, the device surface would be passivated to reduce the surface leakage current and increase the breakdown voltage. This would increase the MTTF and potentially even change the failure mechanism to one in the bulk. When such devices become available, this methodology will be appropriate to characterise their

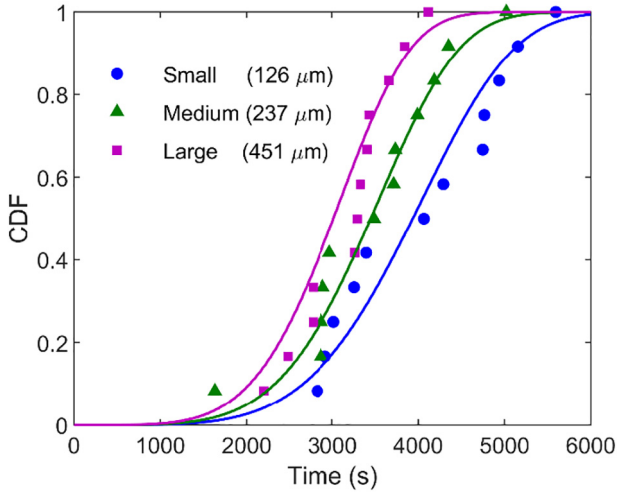

Fig. 4. The cumulative distributions of each of the three device sizes are shown with the symbols. The curves are the step stress Weibull distributions with the average parameter set of Table 1 and differing only by the periphery scaling factor.

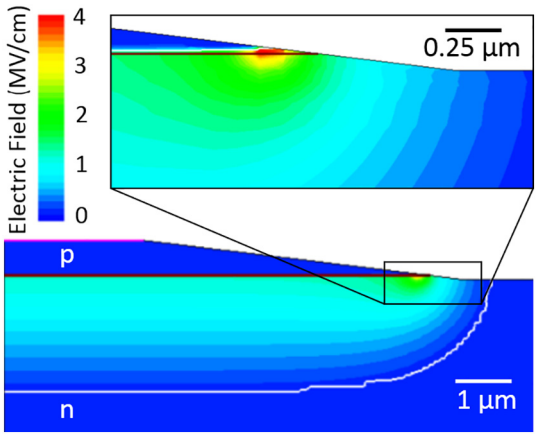

Fig. 6. Simulation of the electric field in the device at a reverse bias of 230 V. The peak electric field of 4 MV/cm is internal but near the surface at the base of the bevel. Surface roughness over the junction would reduce the reverse bias required to attain a 4MV/cm peak electric field.

reliability.

7. Conclusion

The first lifetime estimations of vertical bulk GaN pn diodes have been presented. The results indicate the failure in this case is surface related despite the vertical device geometry. Thus, the lifetime of the device is not limited by the material properties but the device design. The MTTF of these devices was shown to depend only on the length of the device periphery. A MTTF of 10 years at a reverse bias of 260 V was estimated for the smallest device. However, a large variability was seen between devices leading to a very short 1% failure time.

B. Rackauskas acknowledges funding from the UK EPSRC. Supporting data available at doi.org/10.5523/bris.7qywrneti4ig2j2png6cvpf3m.

References

[1] K.J. Chen, O. Haberlen, A. Lidow, C. lin Tsai, T. Ueda, Y. Uemoto, Y. Wu, GaN-on-Si power technology: devices and applications, IEEE Trans. Electron Devices 64 (3) (Mar. 2017) 779–795, https://doi.org/10.1109/TED.2017.2657579.

[2] Y. Zhang, D. Piedra, M. Sun, J. Hennig, A. Dadgar, L. Yu, T. Palacios, High-performance 500 v quasi- and fully-vertical GaN-on-Si pn diodes, IEEE Electron Device Lett. 38 (2) (2017) 248–251, https://doi.org/10.1109/LED.2016.2646669.

[3] H. Ohta, N. Kaneda, F. Horikiri, Y. Narita, T. Yoshida, T. Mishima, T. Nakamura, Vertical GaN p-n junction diodes with high breakdown voltages over 4 kV, IEEE Electron Device Lett. 36 (11) (2015) 1180–1182, https://doi.org/10.1109/LED.2015.2478907.

[4] I.C. Kizilyalli, T. Prunty, O. Aktas, 4-kV and 2.8-mΩ-cm^2 vertical GaN p-n diodes with low leakage currents, IEEE Electron Device Lett. 36 (10) (Oct. 2015) 1073–1075, https://doi.org/10.1109/LED.2015.2474817.

[5] K. Nomoto, B. Song, Z. Hu, M. Zhu, M. Qi, N. Kaneda, T. Mishima, T. Nakamura, D. Jena, H.G. Xing, 1.7-kV and 0.55-mΩ cm^2 GaN p-n diodes on bulk GaN substrates with avalanche capability, IEEE Electron Device Lett. 37 (2) (Feb. 2016) 161–164, https://doi.org/10.1109/LED.2015.2506638.

[6] I.C. Kizilyalli, A.P. Edwards, H. Nie, D. Disney, D. Bour, High voltage vertical GaN p-n diodes with avalanche capability, IEEE Trans. Electron Devices 60 (10) (Oct. 2013) 3067–3070, https://doi.org/10.1109/TED.2013.2266664.

[7] Z. Hu, K. Nomoto, B. Song, M. Zhu, M. Qi, M. Pan, X. Gao, V. Protasenko, D. Jena, H.G. Xing, Near unity ideality factor and Shockley-Read-Hall lifetime in GaN-on-GaN p-n diodes with avalanche breakdown, Appl. Phys. Lett. 107 (24) (2015), https://doi.org/10.1063/1.4937436.

[8] I.C. Kizilyalli, A.P. Edwards, O. Aktas, T. Prunty, D. Bour, Vertical power p-n diodes based on bulk GaN, IEEE Trans. Electron Devices 62 (2) (2015) 414–422, https://doi.org/10.1109/TED.2014.2360861.

[9] I.C. Kizilyalli, P. Bui-Quang, D. Disney, H. Bhatia, O. Aktas, Reliability studies of vertical GaN devices based on bulk GaN substrates, Microelectron. Reliab. 55 (9–10) (2015) 1654–1661, https://doi.org/10.1016/j.microrel.2015.07.012.

[10] E. Fabris, M. Meneghini, C. De Santi, Z. Hu, W. Li, K. Nomoto, X. Gao, D. Jena, H. G. Xing, G. Meneghesso, and E. Zanoni, "Degradation of GaN-on-GaN vertical diodes submitted to high current stress," Microelectron. Reliab., vol. 88–90, no. May, pp. 568–571, Sep. 2018, https://doi.org/10.1016/j.microrel.2018.06.041.

[11] M. Ruzzarin, M. Meneghini, C. De Santi, G. Meneghesso, E. Zanoni, M. Sun, and T. Palacios, "Degradation of vertical GaN FETs under gate and drain stress," in 2018 IEEE International Reliability Physics Symposium (IRPS), 2018, p. 4B.1–1-4B.1–5, https://doi.org/10.1109/IRPS.2018.8353579.

[12] J.H. Stathis, Percolation models for gate oxide breakdown, J. Appl. Phys. 86 (10) (1999) 5757–5766, https://doi.org/10.1063/1.371590.

[13] E. Zanoni, M. Meneghini, G. Meneghesso, D. Bisi, I. Rossetto, and A. Stocco, "Reliability and failure physics of GaN HEMT, MIS-HEMT and p-gate HEMTs for power switching applications: parasitic effects and degradation due to deep level effects and time-dependent breakdown phenomena," WiPDA 2015 - 3rd IEEE Work. Wide Bandgap Power Devices Appl., pp. 75–80, 2015, https://doi.org/10.1109/WiPDA.2015.7369305.

[14] R.E. Davies, F.E. Gentry, Control of electric field at the surface of P-N junctions, IEEE Trans. Electron Devices 11 (7) (Jul. 1964) 313–323, https://doi.org/10.1109/T-ED.1964.15335.

[15] B. Rackauskas, S. Dalcanale, M.J. Uren, T. Kachi, M. Kuball, Leakage mechanisms in GaN-on-GaN vertical pn diodes, Appl. Phys. Lett. 112 (23) (Jun. 2018) 233501, , https://doi.org/10.1063/1.5033436.

[16] W. Nelson, Accelerated life testing - step-stress models and data analyses, IEEE Trans. Reliab. R-29 (2) (1980) 103–108, https://doi.org/10.1109/TR.1980.5220742.

[17] M.J. Kirton, M.J. Uren, Noise in solid-state microstructures: a new perspective on individual defects, interface states and low-frequency (1/*f*) noise, Adv. Phys. 38 (4) (1989) 367–468, https://doi.org/10.1080/00018738900101122.

[18] Y. Mori, H. Yoshimoto, K. Takeda, R. Yamada, Mechanism of random telegraph noise in junction leakage current of metal-oxide-semiconductor field-effect transistor, J. Appl. Phys. 111 (10) (2012) 104513, , https://doi.org/10.1063/1.4721658.

[19] S. Lombardo, J.H. Stathis, B.P. Linder, K.L. Pey, F. Palumbo, C.H. Tung, Dielectric breakdown mechanisms in gate oxides, J. Appl. Phys. 98 (12) (2005), https://doi.org/10.1063/1.2147714.